Prepared for International Journal of Heat and Mass Transfer

HEAT TRANSFER AND AIR FLOW IN A TRANSVERSE RECTANGULAR NOTCH IN A FLAT SURFACE

By Jay Fox

Lewis Research Center,
National Aeronautics and Space Administration.
Cleveland, Ohio

ABSTRACT

Heat-transfer coefficients, pressure coefficients, and recovery factors on all surfaces of transverse rectangular notches, with length-to-height ratios of $\frac{1}{4}$ to $1\frac{3}{4}$, in a plane surface are reported for air speeds from 160 to 590 ft/sec. Thin, unheated boundary layers beneath a uniform stream ahead of the notch are associated with turbulent cavity flow.

Maximum values of the three coefficients are located near the back edge of the notch. Heat-transfer coefficients are proportional to the free-stream mass velocity raised to the 0.8 power, continuing in a new range of notch geometry the previous controversy with the measurements of Larson and ideas of Charwat. A proportionality, based on few data, is tentatively established between heat-transfer coefficient and notch length raised to the -0.2 power for a given notch geometry; it provides a basis for a non-dimensional correlation. Pressure coefficients are unaffected by speed, except for localized compressibility effects. Recovery factors are independent of speed in the square notch but not in longer notches. Measured velocities and temperatures point out the inadequate treatment by existing theories of the major resistance to heat transfer at the surface.

NOMENCLATURE

C_p, static-pressure coefficient, $(p - p_r)/\left(\rho_r U_r^2/2\right)$;

c, specific heat of air at constant pressure;

H, notch height;

h, local heat-transfer coefficient, q_w/t_w;

k, thermal conductivity of air;

L, notch length;

M, Mach number;

p, static pressure;

q_w, heat liberated at surface per unit time and area;

R, recovery factor, $1 - (t_s - t_a)/\left(U_r^2/2c\right)$;

T, temperature group $(tk_s/q_w)(\rho_r U_r/\mu_s)^{0.8}$, $ft^{0.2}$;

t, temperature <u>rise</u> due to heating, Fahrenheit degrees;

t_a, unheated surface temperature, deg F;

t_s, stagnation chamber temperature, deg F;

U, velocity, ft/sec;

W, heat-transfer group, $(h/k_s)(\mu_s/\rho_r U_r)^{0.8}$, $ft^{-0.2}$;

$\overline{W}$, dimensionless heat-transfer group, $(hL/k_s)(\mu_s/\rho_r U_r L)^{0.8}$;

X, distance from front side of notch, in.;

X_1, distance along periphery of notch from back edge, in.;

Y, distance above bottom of notch, in.

Greek symbols

δ, boundary-layer thickness;

μ, viscosity;

ρ, density.

Subscripts

e, edge of free stream bordering upon free shear layer;

f, heat-transfer quantity on flat plate;

r, reference location 0.25 in. ahead of notch;

s, stagnation chamber;

w, surface.

INTRODUCTION

A transverse rectangular notch that is introduced into a plane surface causes little change to a uniform free stream that is flowing past the cutout, if the length of the cavity in the direction of the free-stream flow is not too great compared to the height. A shear layer like that of a free jet boundary forms over the cavity and borders the external potential flow. It widens from the front to the back of the notch, and part of this free shear layer is deflected into the notch at the back edge, giving rise to a flow in the notch. In atmospheric wind tunnel experiments, such as the present investigation, this cavity flow is highly turbulent.

Measurements of heat transfer in cavities

Short notches with length dimensions L up to $1\frac{3}{4}$ times their height H had not been investigated for thermal flow effects prior to the present investigation, although surface pressure and velocity surveys had been reported by Roshko [1] that seemed to indicate a large eddy was rotating in the square notch, complemented by small vortices in the inner corners. Larson [2] measured the average heat-transfer coefficient to longer notches with L/H of 4.8 or more. In laminar flow, average coefficients were about

56 percent of corresponding coefficients that were measured on models with a straight heated portion in place of a cavity. In turbulent cavity flow, the average coefficient was proportional to the external mass velocity $\rho_e U_e$ (at the edge of the free stream) raised to the 0.6 power, whereas straight-sided models engendered average coefficients that were proportional to $\rho_e U_e$ raised to the 0.8 power, which is the same exponent that is associated with turbulent flat plate flow. An omission, in the report, of model dimensions, which were used in the representation of Reynolds number, and heat-transfer coefficient effectively prevented computation of the coefficient by the reader for purposes of comparison. Qualitative agreement with other investigators is shown by the location of maximum local coefficient of heat transfer at the back end of the cavity.

Pressures on the back end of long rectangular notches ($L/H > 4$) in subsonic turbulent flow were shown by Charwat [3] to increase with increasing notch length, whereas the pressures in the front end were always near the free-stream value ahead of the notch. Local heat-transfer coefficients in long rectangular notches ($L/H > 2$) in turbulent flow at one subsonic stream condition were shown in [4] as a fraction of a reference coefficient measured ahead of the notch, which is a different basis of comparison than that used by Larson. The omission of the reference coefficient, which was not calculable from the reported data, prevented the determination of the magnitude of the local heat-transfer coefficients. However, the trends of the local heat-transfer coefficients were favorably compared to other results in [5].

Pressure and heat-transfer coefficients at one free-stream condition ($M = 1.7$) with presumably turbulent flow in long notches ($L/H > 4$) were presented by Morozov [6]. Both coefficients had the same trend as obtained by Charwat. Heat-transfer coefficients could be compared favorably to the Seban-Fox [5] data for similar L/H values by the scheme presented in the latter report.

Pressure, heat transfer, and recovery factor were measured by Thomann [7] in long rectangular notches ($L/H > 3$) in a supersonic stream, but the admitted inaccuracies in measurement cast doubt on the value of the results.

Seban and Fox [5] presented measurements of pressure, recovery factor, and heat-transfer coefficient on the bottom of two notches, $L/H = 1.84$ and 3.47, in which the back sides were formed by a thin fence on a wind tunnel model that is hereinafter called the fence model and is shown in Fig. 1. The subsonic free stream was adjacent to a turbulent notch flow. The heat-transfer coefficient was proportional to the 0.8 power of free-stream mass velocity, a substantially different exponent from the 0.6 value reported by Larson. The greatest heat-transfer coefficient was found at the rear of the notch as in other investigations.

Concepts about heat transfer in cavities

Salient features of theories that pertain to separated flow and the relation of these theories to reality in the form of experiments are considered briefly as follows.

Crocco-Lees theory [8] is a modification of the integral boundary-layer method of analysis that has recently been successfully applied

[9, 10, 11] to the prediction of pressure in separated regions adjacent to a supersonic free stream, although the analytical formulation is not so restricted. The results of polynomial profile analyses [12, 13] have been only cursorily compared with experimental results.

All of the analyses that have successfully predicted heat transfer or pressure in separated flow are based on the boundary-layer equations of motion, which is remarkable in view of the thick viscous region and especially the sharp corners on the flow boundaries that engender effects not explainable by boundary-layer equations.

Inviscid motion has been considered in relation to cavities, but these efforts [14, 15] are interpreted as academic exercises because of the strong effects of viscosity in real flows.

Squire [16] and Batchelor [17] in their consideration of slightly viscous flow in cylinders and wakes reasoned independently that a constant vorticity existed in the central region of a separated flow that was bounded by shear layers or surfaces. Roshko found some evidence of this feature in a square notch in highly turbulent flow; it led to a description of the flow as a rotating eddy. Similar evidence was found during the present investigation.

Chapman [18] and Korst [19, 20] in laminar and turbulent flow, respectively, have visualized a quiescent cavity of constant temperature and pressure and arbitrary shape bounded by a free shear layer that governs both heat transfer and momentum exchange of the cavity. The Chapman result was that the average heat-transfer coefficient to a cavity

was 56 percent of that to a flat plate as long as the cavity with similar flow conditions; it was verified experimentally by Larson. Korst concluded that heat-transfer coefficient was proportional to mass velocity, a result that disagrees with the turbulent flow experiments of Larson and Seban and Fox. It should be noted that Korst's theory was intended primarily to predict the base pressure behind a step which it does with success in supersonic flow as does the corresponding laminar flow theory by Chapman [21].

Charwat [4] visualized that the heat exchange from a cavity was governed by a vortex in the back corner. This vortex received masses of fluid intermittently from the free shear layer and ejected from downstream after they participated in the vortical motion. The theory predicted the dependence of heat-transfer coefficient upon the 0.6 power of mass velocity that was measured by Larson (but not Seban and Fox) in turbulent flow. The corresponding 0.5 power in laminar flow was also predicted by the theory.

None of the analyses produce a proportionality of heat-transfer coefficient to mass velocity raised to the 0.8 power as measured by Seban and Fox. Their report also showed the major temperature drop in the turbulent flow to be near the surface, a region that is ignored in the analyses. The nonquiescent nature of the notch flow that belies the assumptions of Korst is well-known in turbulent flow from the results of Roshko and Seban and Fox that show velocities near the notch surfaces of the order of 0.4 of the free-stream velocity.

Objective of the present study

The lack of thermal measurements in notches shorter than $\frac{L}{H} = 1\frac{3}{4}$, prompted the present study. In order to test the effect of notch size (as contrasted to geometry) on notch performance, the upper limit of length was set at the same geometric ratio, $\frac{L}{H} = 1\frac{3}{4}$, as existed on the smaller fence model of the Seban-Fox experiment.

MEASUREMENTS OF SURFACE QUANTITIES

In the present experiment, a two-dimensional model that is shown in Fig. 1 spanned the 6-in. width of a 6- by 9-in. wind tunnel and divided the air flow into upper and lower streams, each $2\frac{1}{2}$ in. thick. A virtually uniform free stream was attained over the straight section that terminated at the front side of the rectangular notch that is the subject of this investigation. The notch was 2.05 inches in height, and it could be varied in length in multiples of 0.505 inches by relocating the back side.

Free-stream speeds just ahead of the notch U_r were from 160 fps to 590 fps, as determined by surface pressure measurements and an assumption of isentropic expansion of the flow from stagnation conditions. Stagnation pressure was near atmospheric pressure, while stagnation temperature t_s was near 85 deg F.

Surface heating was effected by electrical dissipation from resistance ribbons that were cemented on the laminated plastic shell and connected in series to provide a substantially constant heating rate on the surfaces of the notch. Average gaps of 0.005 in. separated the 0.500 in. wide ribbons along the periphery except for 0.030-in.-wide gaps at the top of the front side and at the bottom of the back side to accommodate a gasket at the latter

location. Thermocouples located just under the ribbons provided surface temperatures. Surface pressure in the notch was sensed by pressure taps that were installed on an alternate configuration of the model that had no heating ribbons, but did have the same outline as shown in Fig. 1. The surface data are presented in three combinations, pressure coefficient $C_p = \frac{p - p_r}{\frac{1}{2}\rho_r U_r^2}$, heat-transfer group $W = \left(\frac{h}{k_s}\right)\left(\frac{\mu_s}{\rho_r U_r}\right)^{0.8}$, and recovery factor $R = 1 - \frac{t_s - t_a}{U_r^2/2c}$. The stagnation and unheated surface temperatures are represented by t_s and t_a, but in all other cases t refers to the temperature rise due to heating, as, for example, in the heat-transfer coefficient $h = q_w/t_w$.

Accuracies of C_p, W, and R are, respectively, $0.014\left(\frac{1}{2}\rho_r U_r^2\right)$, $0.06W$, and $0.02\left(U_r^2/2c\right)$.

RESULTS FROM THE SURFACE DATA

Surface data from the seven notches that comprise this investigation are shown in Figs. 2 to 6 where the perimeter of the notch, measured in inches, is the abscissa; the front edge is on the left and the back edge on the right. Lines parallel to the ordinate are drawn at the front edge, front (inner) corner, back (inner) corner, and back edge. The front and back sides that form the height of the notch are in all cases 2.05 in., whereas the bottom (width) is an integral multiple of 0.505 in. To the right of the line marking the back edge of the notch, pressure coefficients are shown that were measured on the trailing surface of the model downstream of the notch.

Surface pressure

Most notches show (Figs 2 to 6) large pressure coefficients at the top of the back side. This surface bears the impingement of the cavity flow following its acceleration in the free shear layer by the tractions across the mean dividing streamline. The impinging fluid turns and flows down the back side of the notch toward the bottom where further pressure variations result from the interaction of the cavity flow and the boundaries.

In the following discussion, pressure coefficients are first examined in the square notch, then in the shorter notches, and last in the longer notches. Similar sequences are followed in the discussion of thermal results.

On the square notch that is shown in Fig. 4, the trend of C_p exhibits a certain symmetry on the front side, bottom and the lower portion of the back side; local pressure peaks in the inner corners are nearly equal as are the local minimums at the midpoints of the surfaces of the notch. Most of the magnitudes of C_p are much smaller than the peak value, 0.3, near the back edge. Roshko's results compare well with the present pressure coefficients.

Shorter notches show a decrease in the pressure extremes with decreasing lengths of the notches until no pressure increase due to impingement can be seen in the $L/H = 1/4$ notch. In the bottom of this notch a slight pressure rise can be seen, but otherwise the pressure is nearly uniform, suggesting an analogy to a pressure tap.

Exceptional pressures in the $L/H = 1/2$ notch were recorded at the highest speed; C_p in the bottom rose 0.1 above the lower speed values as did the C_p at the top of the back side in the impingement region. During the recording of these pressures it was noted that the manometers declined during the same intervals that a distinct sound emitted from the tunnel, indicating that a standing sound wave was raising the pressure in the bottom of the notch.

For the same flow conditions and geometry that the effect of sound on pressure was observed here, Krishnaumurty [22] showed by means of Schlieren photographs and hot-wire responses that characteristic frequencies of intense sound emanated from the back edge of rectangular notches. Although surface pressure was not measured in the latter investigation, it is indeed likely that the interaction of sound and pressure is similar in the two experiments.

In contrast to the observable sound-pressure interaction in the $L/H = 1/2$ notch at the highest speed, no unusual effects are reflected in the thermal results at high speed.

Surface pressures shown in Fig. 4 for the $\frac{L}{H} = 1\frac{1}{4}$ notch are lower in the downstream end than those found by Roshko on a similar notch and are markedly lower than those on the square notch. The former disparity may be an influence of the thinner boundary layer ahead of the notch ($\delta = 0.039$ in. compared with Roshko's 0.871 in.), shallower free stream, or smaller notches that were used here.

The C_p on the $\frac{L}{H} - 1\frac{1}{2}$ notch that is shown in Fig. 5 is much different from that measured on the square notch or the $\frac{L}{H} = 1\frac{1}{4}$ notch. In this notch, the large C_p on the back side (maximum $C_p \simeq 1/2$) is greater than that of any of the shorter notches. Through the likelihood that an increased pressure on the notch surface is associated with an increased pressure in the adjacent free stream, a turning outward of the free shear layer that bounds the free stream is suggested ahead of the back edge of the notch. The low pressure at the top of the front side of this notch can likewise be associated with a turning of the free stream into the notch. A turning in the same angular direction is signified by the low pressure that is located just downstream of the notch and shown on Fig. 5 to the right of the back edge line. It is likely that a local separation bubble has formed just behind the back edge of the notch. The distribution of C_p on the $\frac{L}{H} = 1\frac{1}{2}$ notch is much different from that reported by Roshko on any notch.

Pressure coefficients on the $\frac{L}{H} = 1\frac{3}{4}$ notch as reported on Fig. 6 are smaller than those on the $\frac{L}{H} = 1\frac{1}{2}$ notch; similar trends are discernible, but magnitudes are reduced. The maximum pressure coefficient in the notch, 0.3, is comparable to the corresponding coefficient in the square notch, but the remainder of the pressures in the back end are higher in the $\frac{L}{H} = 1\frac{3}{4}$ notch.

On the back side of the $\frac{L}{H} = 1\frac{3}{4}$ notch, C_p is observably higher at high speed. By the same likelihood of common trends of pressure on the notch surface as on the edge of the free stream that was stated before, this change with speed can be ascribed to the compressibility effect in

the free stream that accompanies the greater deflection of the stream into and out of the notch in longer notches. This deflection is associated with a local slowing of the free stream and a corresponding pressure rise that becomes a compression process in high-speed flow. As a result, pressure coefficients rise in high-speed flow when a compression occurs and decrease in a corresponding expansion. This latter effect is evident in the pressure coefficient just downstream of the notch. On the nose of the model the compressive effect was observed in the absence of separation at a location where only the free-stream dynamics can affect the surface pressure.

Pressure coefficients that were measured at two locations in the $L/H = 1.84$ notch that was formed on the fence model of the Seban-Fox experiment are close to the coefficients in the $\frac{L}{H} = 1\frac{3}{4}$ notch of the present investigation when they are placed in geometrically similar locations, as shown in Fig. 6. The comparison supports the idea of geometrically similar notches producing similar pressure performance, but the evidence is not conclusive, since there were only two pressure tap locations in the former notch experiment.

In the notches of this investigation, C_p is substantially independent of speed except in (1) the $L/H = 1/2$ notch at high speed where a resonant effect is evident and in (2) the long notches $\left(\frac{L}{H} = 1\frac{1}{2} \text{ and } 1\frac{3}{4}\right)$ where a trend of C_p with speed exists. No regular variation of C_p with geometry is found, but C_p in the downstream end is large in the long notches in agreement with the trend of existing investigations in longer notches.

Geometric similarity in the pressure performance of notches is verified in nearly all comparisons with other results, the principal discrepancies occurring as deviations from Roshko's results in the $\frac{L}{H} = 1\frac{1}{4}$ and $1\frac{1}{2}$ notches.

Recovery factors

Recovery factors in the square notch, which are displayed in Fig. 4, decrease from a maximum in the impingement region and form an undulating pattern that somewhat resembles the trend of C_p. The maximum recovery factor, 0.8, is lower than that on a flat plate in a uniform stream, 0.89. On the bottom, $R(\simeq 0.6)$ is lower than any that has been measured in longer rectangular cavities by Seban and Fox (minimum $R = 0.65$) or by Morozov (minimum $R = 0.84$), and it is lower than those measured behind a step, as reported in [23] (minimum $R = 0.77$), but it is somewhat higher than the recovery factors that are shown in [24] in a study of a circular cylinder with a trailing splitter plate ($R = 0.43$ to 0.55). Within the limits of experimental accuracy, R may be considered independent of stream velocity U_r.

In the short notches, $L/H = 1/4$ and $1/2$, R is near 0.7, which is higher than that observed in those wider notches, $\frac{L}{H} = \frac{3}{4}$, 1, and $1\frac{1}{4}$, that appear in Fig. 4. The local peak in R on the back side of the short notches near the bottom is apparently due to conduction of heat from the warm interior of the model at a location that has a small heat-transfer coefficient but a good conduction path through the model structure. The internal temperature of the model is probably near the recovery temperature on a flat plate, corresponding to R near 0.89, due to the extensive surface of the model that is exposed to the free stream.

Recovery factors that were measured on the $\frac{L}{H} = 1\frac{1}{4}$ notch (Fig. 4) are higher on the back side and somewhat lower on the rest of the notch than the corresponding R on the square notch. The steep drop in R from the maximum, 0.9, at the top of the back side of the notch suggests that high-energy fluid impinges at the top, but that most of the fluid in the notch is at a low energy level.

In the $\frac{L}{H} = 1\frac{1}{2}$ notch, a high level of R accompanies the unusually high C_p. The recovery factor is substantially higher than on the $\frac{L}{H} = 1\frac{1}{4}$ and 1 notches; in fact, the minimum R, 0.85, is greater than the maximum R on the square notch, 0.81. In the back corner where R exceeds unity, the values are larger than any other in this investigation. A speed effect on R, which was absent in the square notch, is evident on most of the periphery of the $\frac{L}{H} = 1\frac{1}{2}$ notch.

On the $\frac{L}{H} = 1\frac{3}{4}$ notch R is smaller than on the $\frac{L}{H} = 1\frac{1}{2}$ notch but larger than on the square notch. The trend of R with speed is reversed in the $\frac{L}{H} = 1\frac{3}{4}$ notch compared with the trend in the $\frac{L}{H} = 1\frac{1}{2}$ notch; R is smaller on the $\frac{L}{H} = 1\frac{3}{4}$ notch at increased speed, whereas it is larger on the $\frac{L}{H} = 1\frac{1}{2}$ notch at increased speed.

Recovery factors that were measured on the fence model experiment (Fig. 6) agree with the present results at the highest speed; however, the lower speed results do not agree. This effect may be a result of the differing geometries at the back edge of the notch in the two experiments, as shown in Fig. 1.

Morozov [6] reported R between 0.85 and 0.87 on the upstream two thirds of the bottom of an L/H = 4 notch adjacent to a stream with a Mach number of 1.7. These values are somewhat higher than those observed in either the present model or the fence model experiments, and, of course, the stream conditions and geometry are quite different.

There is no regular trend of R with notch geometry; recovery factors are lowest in the nearly square notches, higher in the short notches, and highest in the long notches. No change in R with speed occurs in the square notch, but a change is noted in the $\frac{L}{H} = 1\frac{1}{2}$ and $1\frac{3}{4}$ notches.

Heat transfer

A correlation of heat-transfer coefficient h with mass velocity $\rho_r U_r$ raised to the 0.8 power is achieved at nearly all locations in the several notches, as shown, of course, by substantially constant values of $W = (h/k_s)(\mu_s/\rho_r U_r)^{0.8}$ at several speeds. A major departure exists at the top of the back side where a somewhat smaller exponent is indicated in long notches by smaller values of W at higher speed. In that region the exponent of mass velocity approaches the 0.6 value that was reported by Seban et al. [23] in the separated region behind a step, and it also approaches the same 0.6 exponent that was found by Larson to correlate average heat-transfer coefficient in cavities, some of which had rounded corners.

The reason for the disparity on most of the notch periphery between the results of Larson and the 0.8 exponent that was found in the present experiment and the fence model experiment [5] is not clear. Differences in surface

heating conditions and geometry that were utilized by Larson as compared with the present conditions of experiment, namely, constant temperature on the surface and axisymmetric models as contrasted with the constant heat rate and plane model that were used here, do not appear significant enough to cause the difference between exponents.

Heat-transfer group W in the square notch, as shown in Fig. 4, is greatest at the top of the back side where it is 0.06. The initially rapid decrease in W toward the lower corner can be characterized by a power law dependence of heat-transfer coefficient on the distance from the back edge of the notch. This aspect is considered in a following section.

The direction of decreasing magnitude of group W indicates the general direction of flow along the square notch perimeter to be toward the front edge of the notch from the back edge, which is the same direction that was measured by Roshko at the midpoints of the surfaces that formed a square notch. Flow separation from the surface seems to occur before each of the inner corners followed by an impingement about 0.4 in. away from the corner, as shown by the minor peak in heat transfer at that location. This peak affords an estimate of the extent of the small vortices that Roshko envisaged as rotating in the inner corners in an opposite direction to the main circulative flow in the body of the notch. As a help in establishing relative magnitudes, it is of interest to note that 0.026 is an average value of W over the bottom and forward surfaces of the square notch. The value of 0.026 is, of course, that which exists on

an isothermal flat plate in a uniform air stream at the location where the turbulent boundary layer has a unit reference length, as indicated by the well-known correlation from [25].

General trends of W are similar in the smaller notches, $L/H = 3/4$ and $1/2$, to the trend in the square notch, but little evidence remains of the corner vortices in the $L/H = 1/2$ notch. Somewhat lower values of W in the latter notch suggests that the velocities in that notch are smaller. The similar spatial behavior of heat-transfer measurements in the $L/H = 1/2$ notch as in the $L/H = 3/4$ and 1 notches indicates that the direction of flow along the notch surface is the same in the three notches.

In the $L/H = 1/4$ notch, W on the notch bottom is of the order of 0.01, which is about half of W in the $L/H = 1/2$ notch and about 2/5 of W in the square notch. The maximum value of W is only 0.04 in the $L/H = 1/4$ notch compared with 0.05 in the $L/H = 1/2$ notch and 0.06 in the square notch. Most remarkable is the near-uniformity of W in the bottom of this notch, an indication that there is no mean speed along the surface in that region.

The spatial distribution of W in the $\frac{L}{H} = 1, 1\frac{1}{4}, 1\frac{1}{2}$, and $1\frac{3}{4}$ notches is essentially the same except for a greater W in the back corner in the $\frac{L}{H} = 1\frac{1}{2}$ and $1\frac{3}{4}$ notches. The largest value of W, 0.07, in this investigation is found in the $\frac{L}{H} = 1\frac{1}{2}$ notch at the top of the back side.

An inflection in the trend of W on the bottom of the $\frac{L}{H} = 1\frac{1}{2}$ and $1\frac{3}{4}$ notches about $1\frac{1}{2}$ in. from the front side, exists for reasons that are not

clear. This point plays a major role in the changes that occur in W on the bottom when the sides of the notch ar unheated. A comparison of W with and without side heating in the $\frac{L}{H} = 1\frac{3}{4}$ notch is shown on Fig. 7. In the absence of side heating, a marked increase in W exists in the region in back of the inflection, but not in front.

Fig. 7 also contains values of W from the Seban-Fox fence model [5], with $L/H = 1.84$. Since the present $L/H = 1.72$ notch is 2.05 in. high as compared with the former 0.81-in.-high notch, a basis is established for testing the notion of geometric similarity in heat transfer from notches with unheated sides. Since the fence model results are higher than the present results with unheated sides, geometric similarity in notches fails to produce similar values of the dimensional heat-transfer group W and consideration of alternative correlations is in order.

Notch size can be included in the heat-transfer correlation by forming ratios of $h/h_f = W/W_f$, where $W_f = (h_f/k)(\mu/\rho_r U_r)^{0.8} = 0.037\ L^{-0.2}\ \sigma^{1/3}$ and h_f is the average heat-transfer coefficient on an isothermal flat plate as long as the notch that engenders a turbulent boundary layer. The right side of the equation for W_f follows from the correlation of h_f in [25]. Seban and Fox sought constant values of h/h_f in different notches, but an equivalent method is used here. Before comparison to the present W, the fence model results are first multiplied by a ratio of W_f for the two notches so that they are converted to the W that would be found on an imaginary fence model that is the same size as the present model. The resultant lowering, by 16 percent, of the fence model results brings them into better agreement with their spatial equivalents, the present results in

the $\frac{L}{H} = 1\frac{3}{4}$ notch, as shown in Fig. 7.

Seban and Fox showed, for heat transfer in two fence model notches and also behind a step, that a favorable comparison can be obtained between results formulated into h/h_f, as has likewise been shown in the present comparison.

The improved correlation of W as a fraction of W_f (or equivalently h as a fraction of h_f) is a result of multiplying W by the length of the notch L raised to the 0.2 power. In view of this effect, a new correlation group is proposed using L as the characteristic length, namely,

$$\overline{W} = \frac{hL}{k_s}\left(\frac{\mu_s}{\rho_r U_r L}\right)^{0.8}.$$

This new correlation $\overline{W}$ is dimensionless, and, at the same time, it retains the agreement between results from the fence model and the present model that was discussed previously in connection with ratios of heat-transfer groups W/W_f and displayed in Fig. 7. In addition, there is some evidence that $\overline{W}$ is universal in the sense that the agreement shown by Seban and Fox between results from two fence model notches and behind a step on the basis of h/h_f applies equally to the same results when formulated into $\overline{W}$.

No one length, of course, can specify a flow situation in which several lengths are needed for a complete description. In this instance, the boundary-layer thickness ahead of the notch and the height of the free stream are additional relevant lengths of unknown significance in relation to the notch length. However, the major heat-transfer effects seem, from the limited data at hand, to be a function of the length of a rectangular

notch when the boundary layer is thin compared with H at separation, the flow in the notch is turbulent, and the surface ahead of the notch is insulated, as is the case in all instances of favorable comparison that have been discussed.

An unsuccessful comparison by Seban and Fox with the results of Charwat entailed, in the latter experiment, a thick boundary layer ahead of the notch as well as heat transfer to the surface ahead of the notch. Charwat's emphasis of the importance of boundary-layer thickness compared to H is an indication that the significant length, as far as heat-transfer performance is concerned, varies with flow situation.

Spatial variation of heat-transfer coefficient

Spatial variations of W, especially on the back side of the notches, show a certain degree of similarity. If W is plotted logarithmically as a function of the distance on the back side from the top edge X_1, which is the heated length, Fig. 8 is obtained. Power law relations, which, of course, are evidenced in logarithmic coordinates as straight lines, can approximate the spatial variation between $X_1 = 0.5$ and 1.5 in. Greater heat transfer in the back corner of longer notches is accompanied by flatter slopes in Fig. 8 and a corresponding decrease in the negative exponent of length X_1 that specifies the dependence of heat-transfer coefficient.

The magnitudes of W in the $\frac{L}{H} = 1\frac{1}{2}$ notch, which are about 5 percent greater than in the $\frac{L}{H} = 1\frac{3}{4}$ notch on the back side, separate these results from a general trend of increasing values of W with increasing notch

length. Since W is also greater on the front side of the $\frac{L}{H} = 1\frac{1}{2}$ notch, the heat-transfer performance of this notch is unusual as are C_p and R.

The exceptional behavior of W in the shortest notch ($L/H = 1/4$) is evident in Fig. 8 as a small length ($0.6 < X_1 < 1.1$) for the power law behavior and a large negative slope in the distribution of W.

Some tendency toward a power law behavior in W exists on portions of the bottom and front side of the notches, as shown in the results from the $\frac{L}{H} = \frac{1}{2}$, 1, and $1\frac{3}{4}$ notches in Fig. 8. Negative slopes of W are greater on the bottom and front side than on the back side indicating a greater negative exponent of proportionality on X_1.

Fig. 8 also shows in logarithmic coordinates the unaveraged measurements of W on the back side of the square notch to illustrate the changes in slope and exponent that occur at different speeds within the average distribution. In notches with $L/H = 1/2$ or more, exponents of X_1 on the back side at various speeds range from -0.3 to -0.5 with the smaller negative values occurring in the longer notches. Exponents for the $L/H = 1/4$ notch are near -0.9. Except for the latter notch, exponents of distance are between those that are known for turbulent flow on an isothermal flat plate, -0.2, and for a wall jet, -0.6, as reported in [26].

FLOW MEASUREMENTS

Velocity and temperature traverses in the $\frac{L}{H} = 1$ and $1\frac{3}{4}$ notches at low speed ($U_r \simeq 160$ fps) were accomplished along lines that were normal to the notch bottom. Velocity was measured by a hot-wire anemometer that sensed the magnitude of the velocity including components both normal and

parallel to the notch bottom. The velocity is displayed as a fraction of the local free-stream velocity U_e. Detailed measurements are not shown here, in the interest of brevity, but constant speed lines or contours drawn through the traverse results are displayed in Figs. 9 and 11 to give an improved physical concept of cavity flow. Temperatures in the flow were sensed by a Nichrome-constantan thermocouple that was strung between sewing needles.

Velocity of square notch flow

Roshko's interpretation of square notch flow as being dominated by a large rotating eddy was based on velocity traverses of small extent from the surfaces that were located at the midpoints of the three sides of a square notch. The present traverse in the center of the square notch indicates a similar maximum velocity near the bottom, $\frac{U}{U_e} = 0.34$, and a similar trend to that observed by Roshko. The linear trend extends to a very low value, $U/U_e = 0.04$, at the midheight of the notch, followed by a linear velocity increase to the lower edge of the free shear layer as shown in the constant speed contours of Fig. 9. The small size of the region in Fig. 9 that is bounded by the circular low-speed contours around the center of the notch as well as the near zero speed measured at the center suggest that the fluid near the center does indeed rotate. Separate low-speed regions exist at the top and the bottom of the front side, and an isolated high-speed region is found at the center of the bottom. No indications of a rotating eddy, such as velocities on radii from some center being the same, are found except on the central traverse; rather, there are indications that the

flow along the notch bottom continues from back to front except quite close to the corners, which precludes, by continuity, any rotating motion as a solid body that extends to the surface.

Velocity-ratio contours in the free shear layer at the top of the notch in Fig. 9 indicate the large velocity gradients in the layer by the closeness of the contours. A similarity in the velocity profiles on the Y/X basis that has been used in turbulent shear layer analyses by Goertler [27], Korst [19], and others is detectable at the two forward locations of traverse by passing straight lines through the locations of the velocity ratios $U/U_e = 0.3$ to 0.8. These lines intersect at a point located 0.08 in. (X/L = 0.04) away from the front side of the notch. This point is sometimes called a virtual origin of the free shear layer, but its purpose here is to establish the similarity in form of the first two velocity profiles and, at the same time, to imply that a turbulent free shear layer is established quite close to the front side of the notch. Extending these straight lines to the back traverse locations produces a greater separation between the velocity ratios than exists in the measured profiles; hence, the similarity is not sustained across the notch.

Temperatures in square notch flow

Temperature rise due to heating is displayed in Fig. 10 as isotherms or temperature contours that are identified both as t(deg F) and $T(ft^{0.2})$, where $T = (tk_s/q_w)(\rho_r U_r/\mu_s)^{0.8}$ and is conveniently related to W by the relation $T_w \equiv 1/W$. Values of T_w on the surface are shown in Fig. 10.

Temperatures in the flow are everywhere quite low compared with surface temperatures, which implies that the major resistance to heat transfer is at the surface, as evidenced by the major temperature drop there. The regular increase of surface temperature T_w on the back side in the direction of flow is not paralleled by the trend of flow temperatures near the back side, which increases mostly across the free shear layer and near the bottom. The flow temperature along the bottom increases in the direction of flow to a peak in the low speed zone in the front corner. A similar peak exists at the top of the front side in a separate low-speed region.

Velocity in the $\frac{L}{H} = 1\frac{3}{4}$ notch

Velocity ratios U/U_e are shown as contours in Fig. 11 in the free shear layer. The layer dips farther in this notch at $X/L = 0.67$ than the free shear layer on the square notch, and it subsequently turns outward before the back side of the notch. This motion was related in a previous section to the increased C_p on the back side of this notch compared to C_p in the square notch. This motion was also significant in the rationalization of the increased C_p in this region at high speeds by means of the compression that occurs in the free stream at a turn.

Similarity on a Y/X basis is established in the first two velocity profiles by passing straight lines through $U/U_e = 0.3$, 0.5, and 0.7 and by observing the intersection at $X/L = 0.04$ ($X = 0.16$ in.), about the same location on an X/L basis as in the square notch. The angle of divergence between straight contours through $U/U_e = 0.3$ and 0.7 is

substantially the same in this notch as in the square notch, but the initial similarity in this notch is retained over the length of the free shear layer, in contrast to the square notch, after vertical shifts in coordinates are introduced to line up the traverses toward the back of the notch.

Below the free shear layer velocity gradients are less well defined so that a brief description is adequate to interpret the temperature field in the next section. Velocities in the notch are near $0.15\ U_e$ except adjacent to the bottom where they are directed forward and attain a peak value near $0.4\ U_e$ over the back two-thirds of the bottom. They are smaller however, on the front one-third, especially near the front side. Evidence of vortices was found only on the 1/2 in. adjacent to the corners.

Temperatures in the $\frac{L}{H} = 1\frac{3}{4}$ notch

As in the square notch, t and T are shown in Fig. 11 as isotherms in the $\frac{L}{H} = 1\frac{3}{4}$ notch. Temperatures in the central region of the notch away from the surface and free shear layer are somewhat lower in this notch than in the square notch both in values of t (deg F) and $T(ft^{0.2})$. A temperature peak (or hot spot) exists in the central region of the notch, specifically at $X/L = 0.35$ and $Y = 0.8$ in. A peak at such a location gives the appearance of a source of heat in the flow because of the usual physical concept of heat always diffusing in the direction of declining temperature. Heat transfer is also unusual on the bottom beneath the temperature peak; $W\left(= \frac{1}{T_w}\right)$ shows a local peak and valley there. This

location on the bottom is also the limit of changed values of W that result from not heating the notch sides; W is increased toward the back but changed little toward the front, as shown in Fig. 7. Flow speed along the bottom begins a rapid decline toward the front from this location. All these measurements, however, serve just to identify the site of unusual effects and do not combine to produce a coherent explanation of the flow and thermal phenomena there.

A "valley" of temperature that is revealed by the isotherms just above the back two-thirds of the bottom is associated with the high speed flow, $U \simeq 0.4\ U_e$, which extends forward to the neighborhood of the temperature peak. Flow temperatures near the back side are comparable in magnitude ($T \simeq 5$) and trend to those in the square notch; temperature is nearly uniform over much of the height of both notches. Similar shapes of temperature contours close to the front corner are noted in the two notches, but the temperatures are lower here, as elsewhere, in the $\frac{L}{H} = 1\frac{3}{4}$ notch.

Additional studies of shear on the bottom, pressure-velocity interaction in the notch, pressure and heat-transfer predictions, turbulence intensity, flow visualization and convective heat transport in the free shear layer as well as measurements in the flow of the $L/H = 1/2$ notch, and other measurements that have been discussed but not shown here are available in [28].

SUMMARY

Surface pressure coefficient and recovery factor R are comparable in three groups of notches: short notches ($L/H = 1/4$ and $1/2$), which have nearly uniform pressure and $R \simeq 0.7$ on the bottom; nearly square notches

$\left(\frac{L}{H} = \frac{3}{4}, 1, \text{ and } 1\frac{1}{4}\right)$, which have a nearly symmetrical pressure pattern with peaks in the corners and $R \simeq 0.6$ on the bottom; and long notches $\left(\frac{L}{H} = 1\frac{1}{2} \text{ and } 1\frac{3}{4}\right)$, which have high pressure in the back end and R near 0.85 on the bottom. Pressure coefficients and recovery factors are comparable to existing measurements in a few cases of similar geometry. A variation in recovery factor with speed exists in the $\frac{L}{H} = 1\frac{1}{2}$ and $1\frac{3}{4}$ notches but not in the square notch.

Heat-transfer coefficient is proportional to free-stream mass velocity raised to the 0.8 power at nearly all locations. Peak heat transfer occurs at the top of the back side (W = 0.04 to 0.07) with all surfaces of the notch heated, but moderate values (W near 0.02) are noted elsewhere, except on the shortest notch (L/H = 1/4) where unusually low performance ($W \simeq 0.01$) is obtained in the bottom. Heat-transfer results from the $\frac{L}{H} = 1\frac{3}{4}$ notch are comparable to the Seban-Fox results only after values of W are multiplied by their respective notch lengths raised to the 0.2 power, rendering W dimensionless. A lack of heating on the sides of the $\frac{L}{H} = 1\frac{3}{4}$ notch produces greater values of W only on the rear two-thirds of the notch bottom. Heat transfer on the lower part of the back side of a notch is greater in longer notches, and this effect is accompanied by a changing power law dependence of heat-transfer coefficient on length from the top of the back side.

As anticipated by Roshko, a linear variation of speed with distance from the center of the square notch is found at the midlength, but the

accompanying interpretation of the motion as a solid-body rotation is found to be lacking. Temperatures in the square notch flow are low compared with the surface temperature, implying that the major resistance to heat transfer exists at the notch surface, but the accompanying temperature gradients at a distance from the surface suggest that heat transfer occurs everywhere within the notch flow.

The free shear layer dips farther into the $\frac{L}{H} = 1\frac{3}{4}$ notch than the square notch, as evidenced both by velocity and surface pressure measurements. No evidence of rotating flow was found in the $\frac{L}{H} = 1\frac{3}{4}$ notch, but rather, a strong flow forward along the bottom existed over the rear two-thirds of the notch bottom. An enigmatic temperature peak occurs in the flow at one-third of the notch length and accompanies heat-transfer perturbations at the same location on the bottom of the notch.

ACKNOWLEDGEMENT

The guidance of Prof. R. A. Seban of the University of California, Berkeley, is gratefully acknowledged. Research which produced these results was supported by the National Science Foundation under Grant 17909.

REFERENCES

1. A. Roshko, Some measurements of flow in a rectangular cutout, NACA TN 3488 (1955).

2. H. K. Larson, Heat transfer in separated flows, J. Aerospace Sci., 26, 731 (1959).

3. A. F. Charwat, J. N. Roos, C. F. Dewey and J. A. Hitz, An investigation of separated flows. Pt. I - The pressure field, J. Aerospace Sci., 28, 457 (1961).

4. A. F. Charwat, C. F. Dewey, J. N. Roos and J. A. Hitz, An investigation of separated flows. Pt. II. Flow in the cavity and heat transfer, J. Aerospace Sci., 28, 513 (1961).

5. R. A. Seban and J. Fox, Heat transfer to the air flow in a surface cavity, Proceedings of the 1961-62 Heat Transfer Conference, p. 426, ASME (1963).

6. M. G. Morozov, Interaction between a supersonic stream and a rectangular depression on a flat plate, Soviet Phys.-Tech.Phys., 3, 144 (1958).

7. H. Thomann, Measurements of heat transfer and recovery temperature in regions of separated flow at a Mach number of 1.8, Aero. Res. Inst. Sweden, Report 82 (1959).

8. L. Crocco and L. Lees, A mixing theory for the interaction between dissipative flows and nearly isentropic streams, J. Aero. Sci., 19, 649 (1952).

9. J. Vasiliu, Pressure distribution in regions of step-induced turbulent separation, J. Aerospace Sci., 29, 596 (1962).

10. H. S. Glick, Modified Crocco-Lees mixing theory for supersonic separated and reattaching flows, J. Aerospace Sci., 29, 1238 (1962).

11. J. Rom and M. Victor, A theoretical and experimental determination of the base-pressure behind a two-dimensional backward facing step in a laminar supersonic flow, p. 71, Proceedings of the 5th Israel Annual Conference on Aviation and Astronautics, Jerusalem Academic Press, Ltd. (1963).

12. W. O. Carlson, Heat transfer in laminar, separated and wake flow regions, Proceedings 1959 Heat Transfer Fluid Mech. Inst., p. 140, Stanford Univ. Press (1959).

13. M. H. Bloom, On moderately separated viscous flows, J. Aerospace Sci., 28, 339 (1961).

14. J. D. Cole, Note on the effect of circulation in heat transfer, Rand Corp. Res. Memo. 1351 (1954).

15. H. Serbin, Flow induced by a cavity in a supersonic stream, J. Aerospace Sci., 28, 247 (1961).

16. H. B. Squire, Note on the motion inside a region of recirculation (cavity flow), J. Roy. Aero. Soc., 60, 203 (1956).

17. G. K. Batchelor, On steady laminar flow with closed streamlines at large Reynolds numbers, J. Fluid Mech., 1, 177 (1956).

18. D. R. Chapman, A theoretical analysis of heat transfer in regions of separated flow, NACA TN 3792 (1956).

19. H. H. Korst, A theory for base pressures in transonic and supersonic flow, J. Appl. Mech., 23, 593 (1956).

20. H. H. Korst and W. L. Chow, Compressible non-isoenergetic two-dimensional turbulent ($Pr_t = 1$) jet mixing at constant pressure - auxiliary integrals - heat transfer and friction coefficients for fully developed mixing profiles, Univ. Ill., ME-TN-392-4, OSR-TN-59-380 (1959). Also ME-TR-392-5 (1959).

21. D. R. Chapman, D. M. Kuehn and H. K. Larson, Investigation of separated flows in supersonic and subsonic streams with emphasis on the effect of transition, NACA Report 1356 (1958).

22. K. Krishnamurty, Acoustic radiation from two-dimensional rectangular cutouts in aerodynamic surfaces, NACA TN 3487 (1955).

23. R. A. Seban, A. Emery and A. Levy, Heat transfer to separated and reattached subsonic turbulent flows obtained downstream of a surface step, J. Aerospace Sci., 26, 809 (1959).

24. R. A. Seban and A. M. Levy, The effect of a downstream splitter plate on the heat transfer from a circular cylinder normal to an airstream, WADC TR 57-479 (1957).

25. H. A. Johnson and M. W. Rubesin, Trans. ASME, 71, 447 (1949).

26. R. A. Seban and L. H. Back, Velocity and temperature profiles in a wall jet, Int. J. Heat Mass Transfer, 3, 255 (1961).

27. H. Goertler, ZAMM, 22, 244 (1942).

28. Jay Fox, Heat transfer in separated flow, Ph. D. Thesis, Univ. Calif., Berkeley (1963); also Univ. Microfilms, Inc., Ann Arbor, Mich.

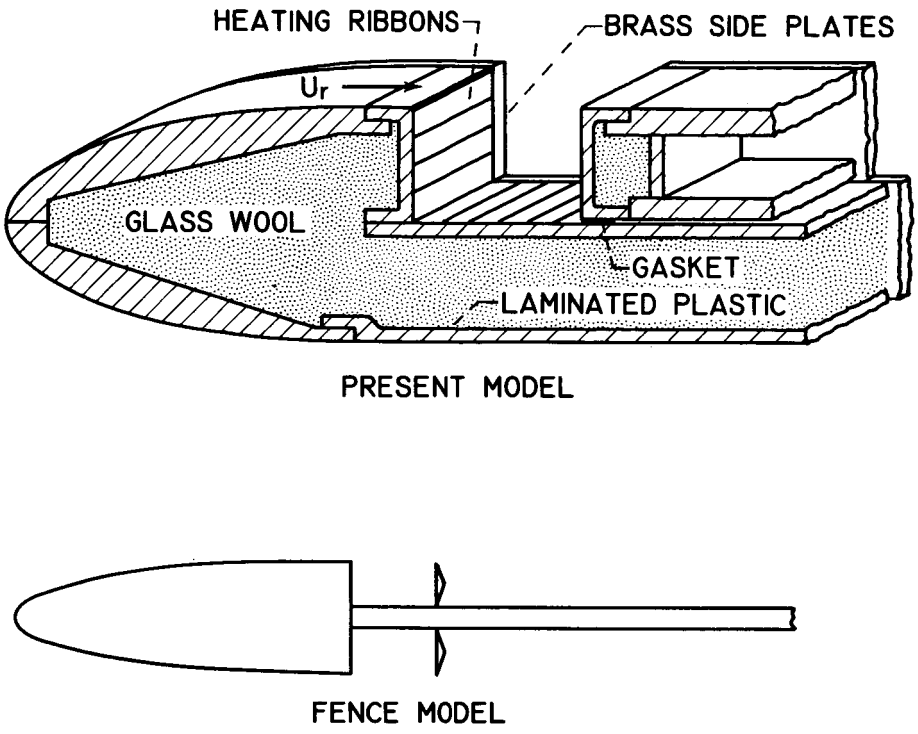

Fig. 1. - Present model and Seban-Fox fence model.

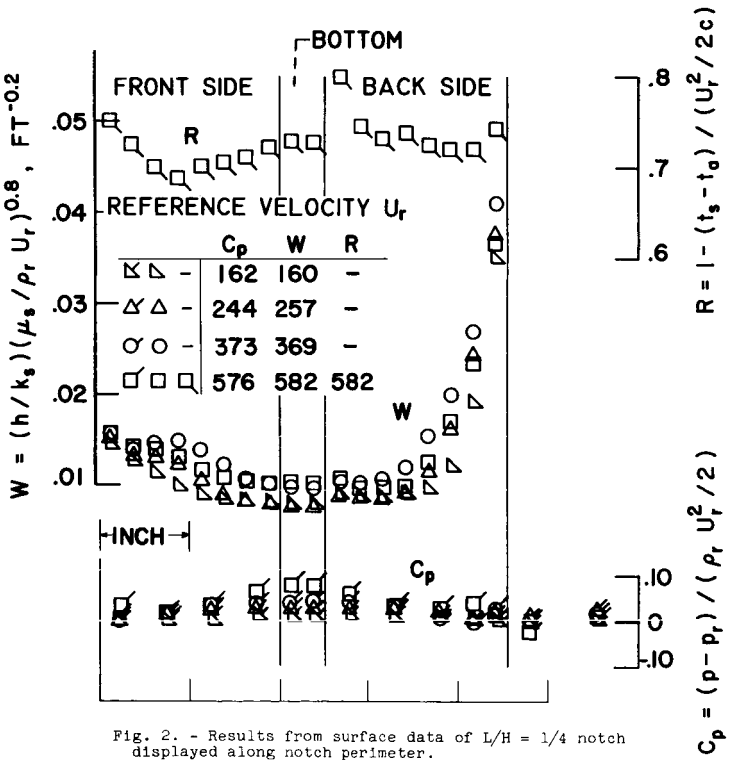

Fig. 2. - Results from surface data of L/H = 1/4 notch displayed along notch perimeter.

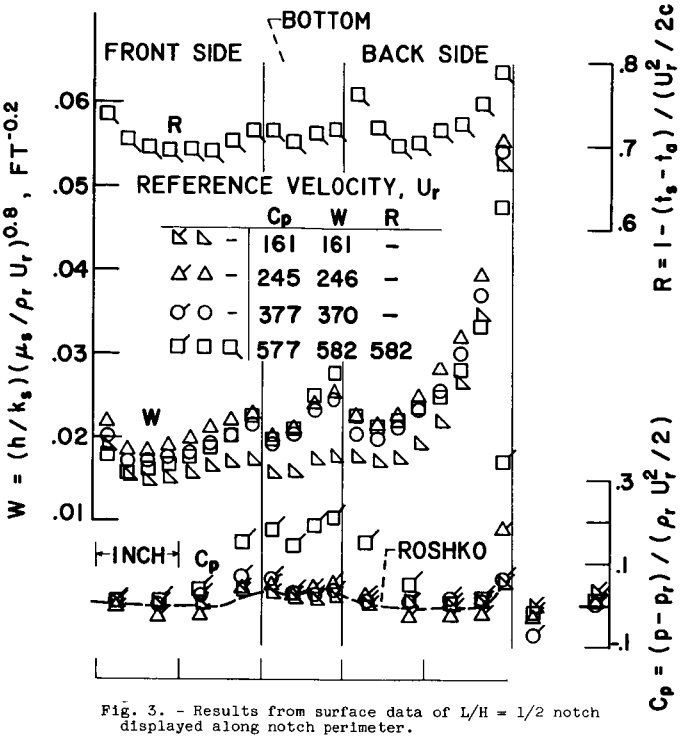

Fig. 3. - Results from surface data of L/H = 1/2 notch displayed along notch perimeter.

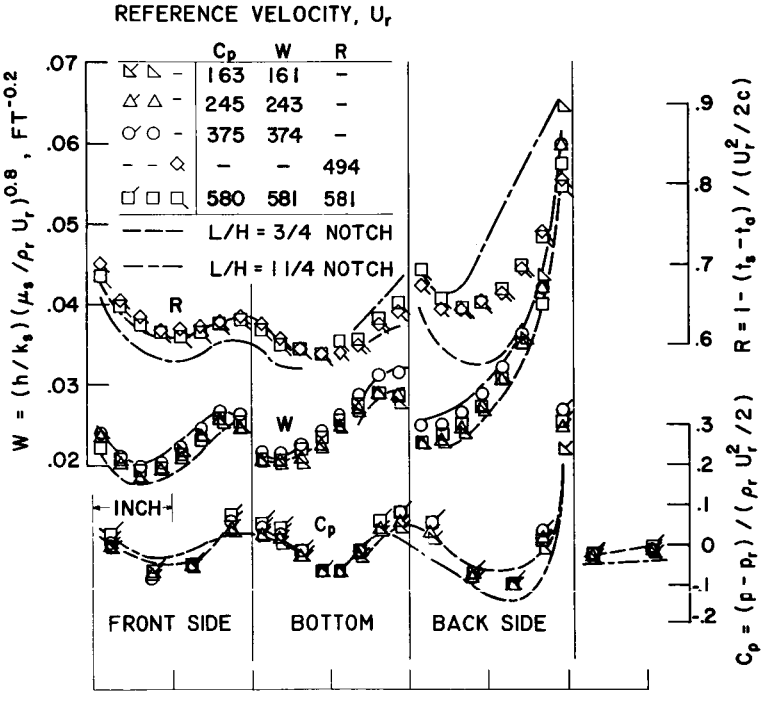

Fig. 4. - Results from surface data of L/H = 1 notch and averaged results from L/H = 3/4 and 1 1/2 notches.

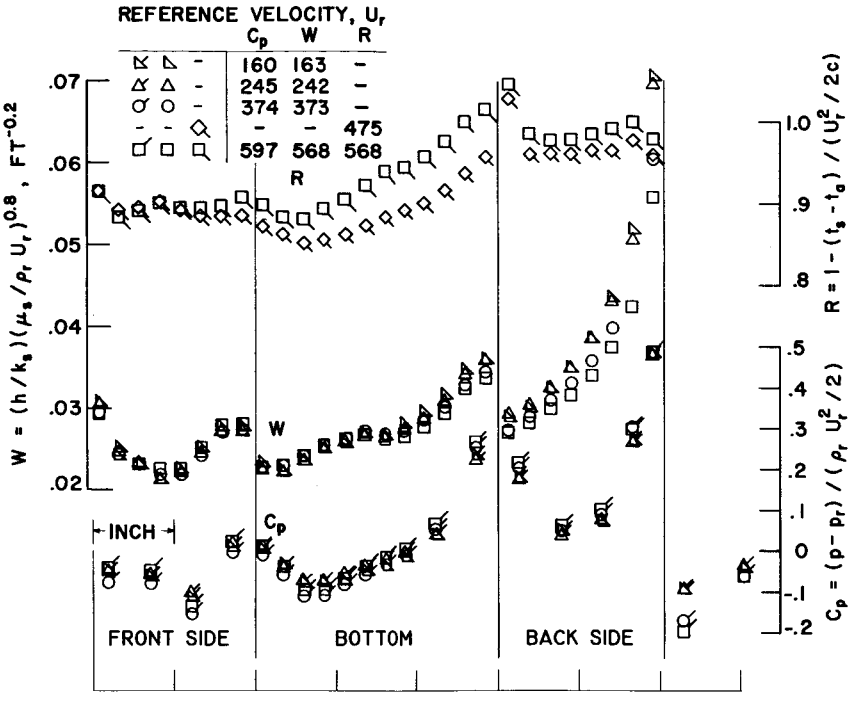

Fig. 5. - Results from surface data of L/H = 1 1/2 notch displayed along notch perimeter.

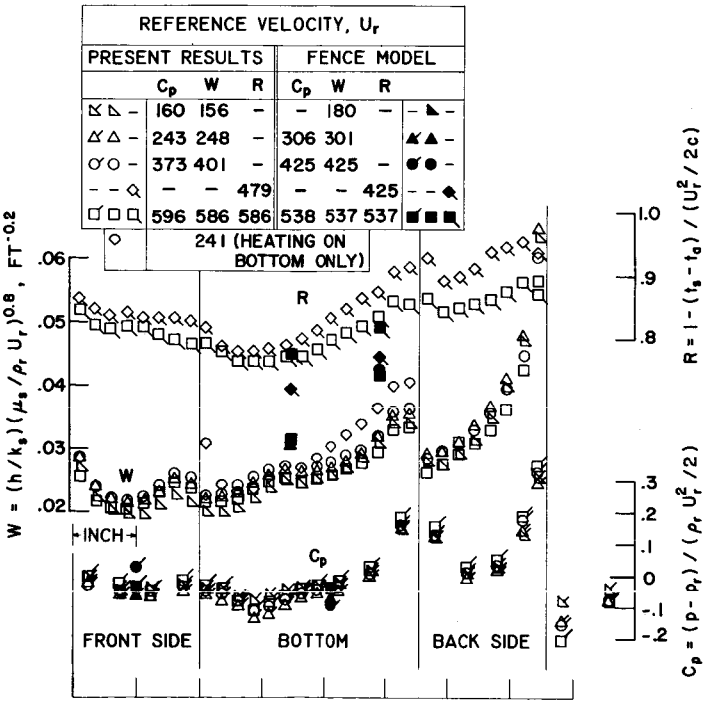

Fig. 6. - Results from surface data of L/H = 1 3/4 notch and Seban-Fox fence model.

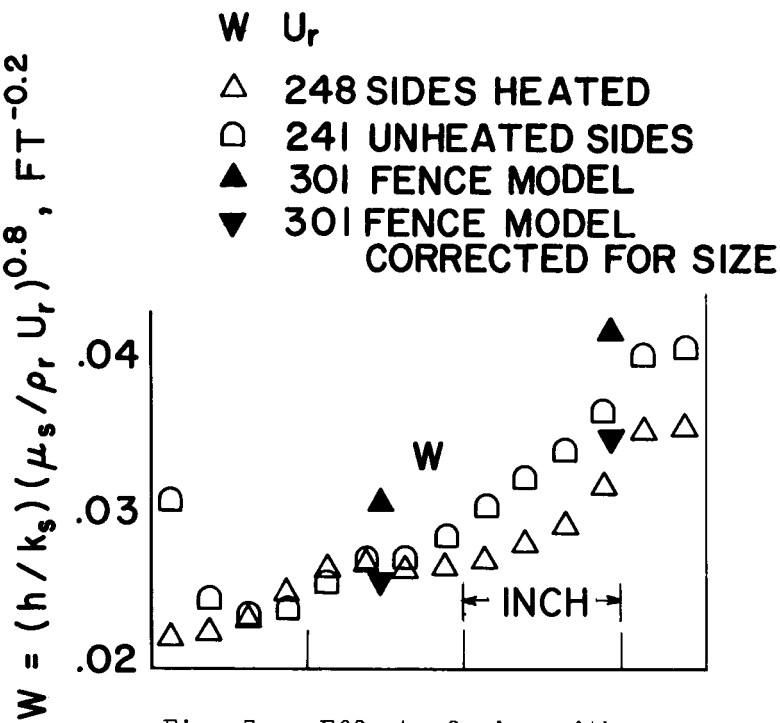

Fig. 7. - Effect of size with unheated sides on heat transfer on bottom of L/H = 1 3/4 notch.

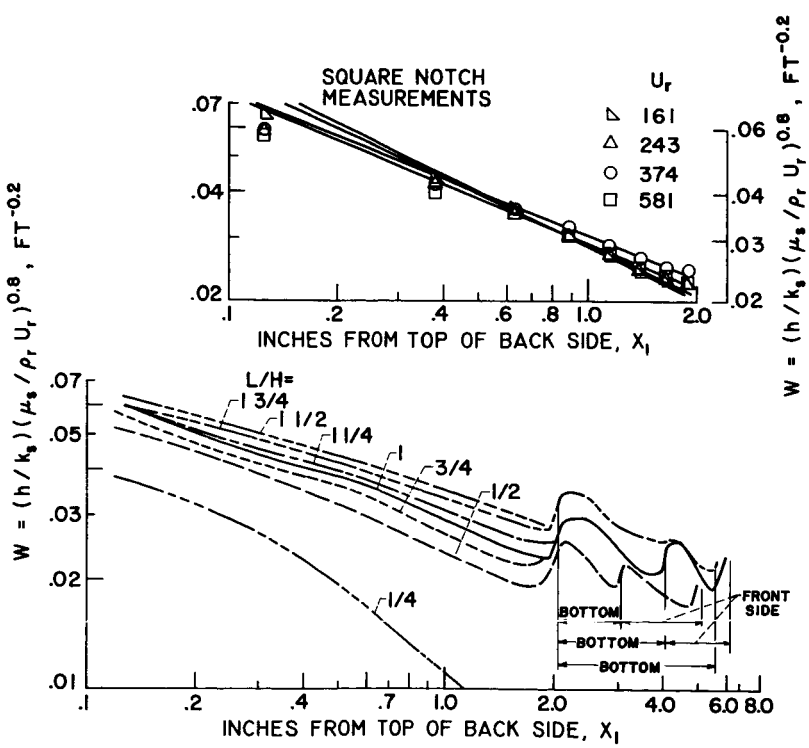

Fig. 8. - Average heat-transfer results along notch perimeter from back edge. In the insert, speed effects on power law behavior in square notch.

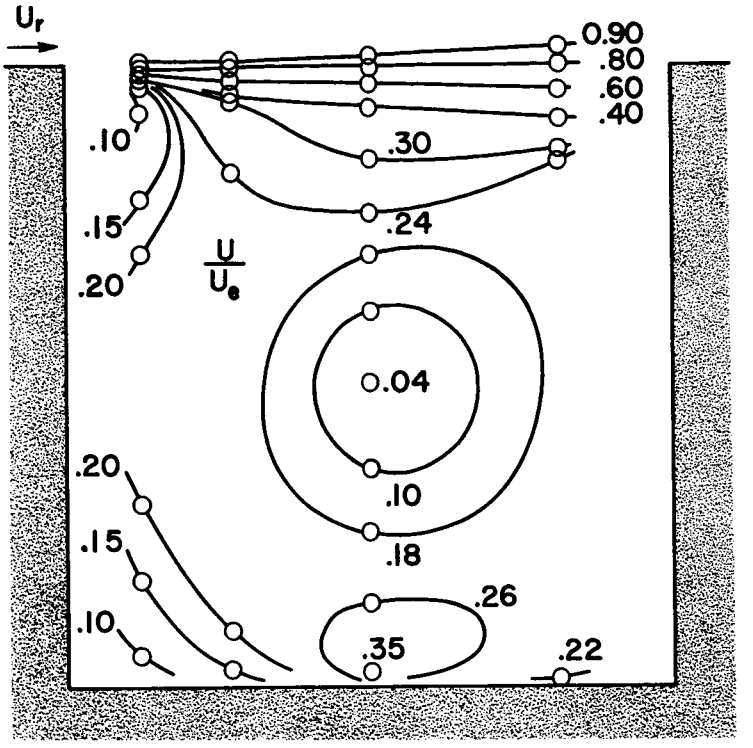

Fig. 9. - Velocity ratio contours within square notch. Lines of constant velocity ratio drawn through circled measurements.

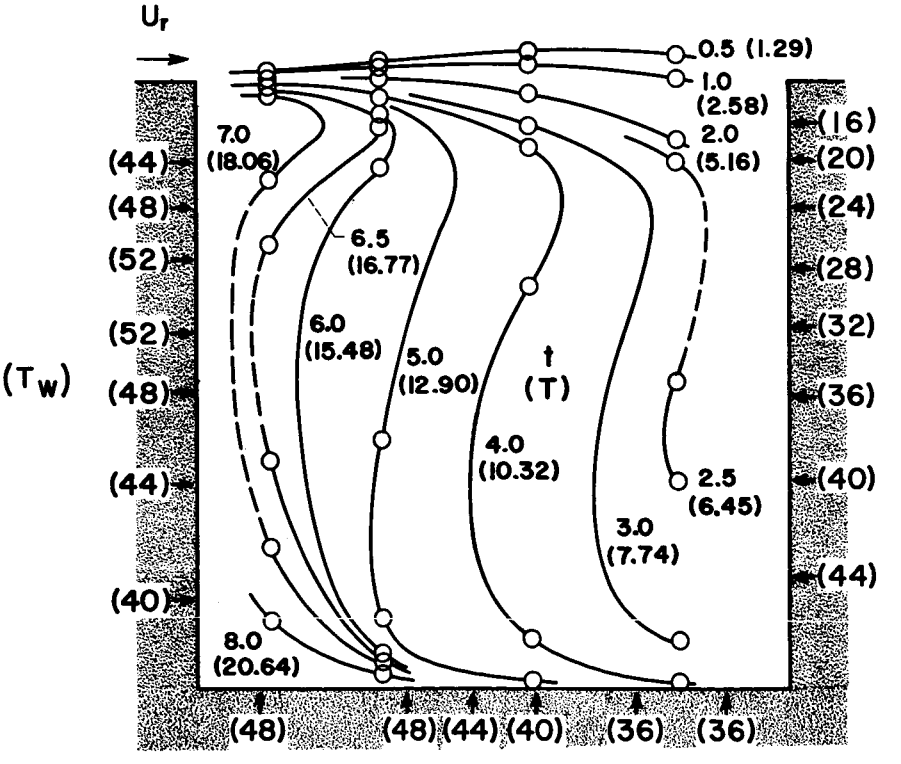

Fig. 10. - Temperature contours in square notch. Lines of constant temperature rise due to heating drawn through circled measurements.

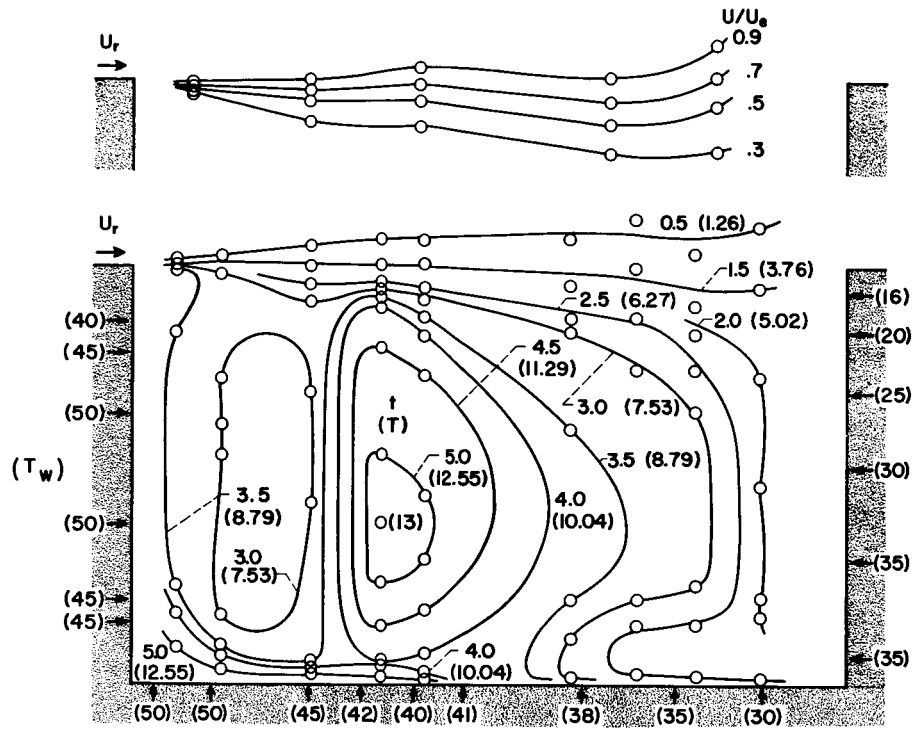

Fig. 11. - Temperature and velocity contours in L/H = 1 3/4 notch.